Available online www.jsaer.com

***Journal of Scientific and Engineering Research*, 2022, 9(7):92-104**

Research Article

ISSN: 2394-2630
CODEN(USA): JSERBR

Study of the textural properties and nitrogen adsorption capacity of activated carbons based on Oryza Sativa bran pretreated with soda

Clément K. Balogoun[1,2,3], Ibrahim Tchakala[2], Sey-Laye M. Alfa-Sika[2,4], Kodom Tomkouani[2], Moctar L. Bawa[2]

[1]Applied Chemistry Study and Research Laboratory, Polytechnic School of Abomey-Calavi University, Abomey- Calavi, Benin
[2]Laboratory of Applied Hydrology and Environment, Faculty of Sciences, University of Lomé, BP 1515, Togo
[3]Water Science and Technology Laboratory, Polytechnic School of Abomey-Calavi University, Abomey-Calavi, Benin
[4]Faculty of Science and Technology, University of Kara, Togo
Email: balck@yahoo.fr

Abstract In this work, the textural properties of activated carbons prepared chemically with phosphoric acid H_3PO_4 at 25%, on the basis of pre-treated rice bran were studied. The pre-treatment of the rice bran consisted in its leaching with 1N and 2N sodium hydroxide solution. Xp impregnation ratios ranging from 1.5 to 4 grams of acid per gram of precursor were applied. The samples of the two series of activated carbons, SR_1N and SR_2N obtained were subjected to the adsorption of iodine and nitrogen N_2. From the adsorption isotherms of N_2 on the activated carbons, the main texture parameters (specific surface, porosity, pore size distribution and average pore diameter) were determined. Four calculation models: B.E.T. equation, t-plot method, B.J.H. method and the one developed by Horvath-Kawazoe (HK) were used. These measurements and calculations show that the specific areas B.E.T specific surface areas are between 661.3 and 1688.4 m^2/g with pore volumes ranging from 0.652726 to 1.400319 cm^3/g. In addition, the activated carbons have a dominant mesoporous character with average pore diameters between 2.902 and 3.948 nm.

Keywords Adsorption isotherms, BET, t-plot, BJH and Horvath-Kawazoe (HK)

Introduction

The importance of activated carbon lies in the diversity of its use (or application) and makes it the most coveted adsorbent. Indeed, activated carbon is used in several fields such as : environmental protection, food processing and pharmaceutical industries, for the removal of a wide variety of chemicals, both organic and metal ions, in the liquid or gas phase [1–4]; electrochemistry for the manufacture of electrodes, super capacitors, batteries and cartridges, energy storage in the form of gases (e.g. hydrogen) [1, 4, 5]; and catalysis (as direct catalysts or catalyst supports for a variety of reactions [6, 7]. These multiple uses of activated carbon are related to its morphology, which are: its physical or textural properties (specific surface, nature and size distribution of the pores) and its surface chemistry. Compared to other adsorbents, such as activated aluminium, aluminophosphates, silica gel, clay and porous polymers, AC has a number of advantages including: its mechanical, heat and radiation resistance, and its stability in acidic and basic solutions [8, 9]. These materials are also cost-effective from a regeneration perspective. Its enormous application potential

combined with its relatively low cost make it the most coveted adsorbent on the market for these types of materials, despite the recent appearance of a competing adsorbent, zeolite. Indeed, zeolite has the same properties as activated carbons in terms of conductivity and heat resistance but with a very narrow pore size distribution. Global demand for activated carbon is forecast to grow at 6% per year for the period 2017-2020 [10, 11]. According to "Global Activated Carbon Market Forecast and Opportunities, 2016", the activated carbon market could reach $3 billion in 2020 in revenue. The physical properties and chemical composition of the precursors, as well as the activation methods and conditions, determine the final pore size distribution and adsorption properties of activated carbon [12–14]. For this reason, the surface area or pore volume of activated carbon can vary considerably from one species to another. The gas adsorption capacity of coals has been known for a long time [15]. It is high for this adsorbent due to its porous characteristics such as specific surface, pore volume and pore size distribution [15]. By studying the physical and chemical properties of carbon atoms synthesized from xylose, cellulose, Kraft lignin (all lignocellulosic precursors) and by activation with H_3PO_4 [14], have shown that for the same preparation conditions, these properties vary from one precursor to another. Also, these same authors [14] reported that an activated carbon whose precursor is of low density, such as wood or lignite, has little microporosity. On the other hand, activated carbons produced from fruit stones, which have a higher density, are very microporous [10]. In addition, the mode of activation (chemical, physical and chemical/physical), the activating agent, the carbonization temperature, etc. are all factors and/or parameters that determine the porous texture of a coal [16–18].

In Benin, one of the main agricultural sectors that generates significant quantities of lignocellulosic residues is rice (*Oryza Sativa*). Indeed, from 2008 to 2015, rice production in Benin increased from 112,705 tonnes to more than 245,000 tonnes of rice in 2015 [19]. Benin has two rice mills, one in Glazoué (in the centre of the country) and the other in Malanville (in the north). Two types of residues come from rice production. These are bran and straw. Straw is often burnt on site or used as a source of domestic energy for cooking. Bran is used as a feed additive in animal production. Both residues, and particularly rice bran, can also be used for the production of activated carbon. Rice bran represents about 20% of the total weight of unhulled rice [20].

In the present study, we determined the pore texture and specific surface areas of three grades of chemically activated carbon with H_3PO_4. The chemical activation is preceded or not by a pre-treatment with soda solution at different concentrations. The objective of this work is to determine the textural properties of local rice-based activated carbons, prepared chemically at H_3PO_4. Specifically, this will involve to assess the effect of pre-treatment and soda concentration on the iodine value and the specific surface, the development of the pores of the activated carbons obtained and the distribution of activated carbon pores.

2. Materials and methods

2.1 Materials and methods of preparation

2.1.1. Materials

The rice bran comes from the Glazoue rice mill in central Benin. It is obtained by mechanically grinding the whole rice grains. Table 1 shows the heteroatom composition and proportions of the biopolymers of this precursor.

Table 1: Characterization of the precursor (rice bran)

Elemental composition (%)		**Proportions of biopolymers (%)**	
Carbon	43.4	Lignin	27.4
Hydrogen	5.4	Cellulose	33.8
Oxygen	41.3	Hemicellulose	21.7
Nitrogen	0.7	Mould	6.1
-	-	Ash	10.8

Photo 1: *Rice seeds (Orysa sativa)*

Photo 2: *Rice bran (Orysa sativa)*

The rice bran was washed with tap water and then rinsed with distilled water to remove dust and other impurities. It was then dried at 110°C in the Heraeus INSTRUMENTS oven for 24 hours. From this raw material, three series of activated carbon are prepared: SR1N and SR2N.

2.1.2 Methods of preparation

The process consists of three steps according to the series. The first step consists of soaking the rice bran with the 1N or 2N NaOH solution to obtain CA, SR1N or SR2N respectively. This mixture made for a ratio of 1:8 (m/v) was then dried at 110 °C in an oven. The dried bran was washed several times with distilled water until a filtrate with a constant pH equal to that of the distilled water was obtained, then dried at 110°C for 24 hours. The second step is the impregnation with the 25% orthophosphoric acid solution ($V_{acide}/V_{solution}$), by heating under reflux for two hours. The concentrated phosphoric acid is 85% with a density of 1.71 $kg.L^{-1}$. The mixture of acid solution and rice bran, after heating to reflux, is subjected to oven drying at 110 °C. The particles thus obtained are carbonized in a furnace (Nabertherm LE14 C290/11) at 500 °C. After cooling to room temperature, the activated carbon was washed first with a 0.1 N hydrochloric acid HCl solution and rinsed several times with hot distilled water.

2.2 Analysis

2.2.1 Iodine value of activated carbons

The iodine value of the prepared activated carbons was determined using ASTM D4607-94, (ASTM D4607-94, 2006). The amount of adsorbed iodine (in mg) per gram of activated carbon with a residual iodine concentration of 0.02 N, represents the iodine value (ASTM D4607-94 2006). The method is as follows:

a. 50 mL of an iodine solution (0.1 N) is added to three different masses of activated carbon samples contained in three 250 mL Erlenmeyer flasks, initially wetted with 5 mL of 5% HCl;

b. the contents of the vial are shaken vigorously for 30 (± 1) seconds and then filtered rapidly through Whatman pleated filter paper, No 2V.

c. 25 mL of the filtrate is titrated with 0.1 N sodium thiosulphate solution until the solution becomes pale yellow. 2 mL of a starch indicator solution (1 g/l) was added, and the titration was continued with sodium thiosulphate until the solution became colourless. The volume of thiosulphate consumed is given as V2.

d. the quantity of iodine adsorbed, expressed in mg per gram of activated carbon for each of the three masses, i.e. X/m CA

$$\frac{X}{m_{CA}} = \frac{126{,}9044}{m_{CA}}(50.N_1 - 55.C_r)$$

with

- C_r, the residual iodine concentration of the filtrate;
- N_1, the normality of the iodine solution;

- N_2, the normality of the thiosulphate solution;
- V, the volume of the titrated filtrate (V = 25 mL)

To determine the iodine value, the curve X/mCA = f(Cr) is drawn using the three masses. This curve is a straight line. The iodine value corresponds to the value X/mCA for which the residual iodine concentration is 0.02 N.

2.2.2 Texture characterization: specific surface area and pore structure

The texture of activated carbons was determined from their N adsorption/desorption isotherm data2 at 77 K (-196 °C). These data are obtained using an ASAP 2020 M multi-gas porosimeter.

The specific surface area (S_{BET}) was determined using the Brunauer, Emmett and Teller (B.E.T) equation, [21], in its linear form,

$$\frac{P/P_0}{V_{ads}(1-P/P_0)} = \frac{1}{V_{ml}.C_{BET}} + \frac{C_{BET}-1}{V_{ml}.C_{BET}}.\frac{P}{P_0} \qquad \text{Equation 1}$$

V_{ads}: volume of gas adsorbed under pressure P;

P_0: saturation vapour pressure of the gas at the temperature of the experiment;

V_{ml}: volume of gas required to completely cover the surface of a monolayer of gas; C_{BET}: characteristic constant of the solid/gas system studied (B.E.T. constant).

3. Results and Discussions

In liquid media, iodine is one of the model molecules used to assess the textural properties of an activated carbon. The application of the theoretical models developed by certain authors to the data on the adsorption of N_2 at 77 K on the activated carbons developed, gave the physical characteristics (specific surface, volume and distribution of the size of the pores) grouped together in the table 2.

Table 2: Specific surface, volume and distribution of the size of the pores

CA	Xp	I_2 (mg/g)	B. E. T			B. J. H	t-Plot	Vμ/VT (%)
			SBET ($m^2 g^{-1}$)	V_T (cm^3g^{-1})	Dp (nm)	Vméso (cm^3g^{-1})	Vμ (cm^3g^{-1})	
SR2N	1.5	822	1181.4352	1.040356	3.52235	0.711948	0.201365	19.355
SR2N	2.0	786	661.2821	0.652726	3.94825	0.421783	0.178166	27.3
SR2N	2.5	893	917.6947	0.665744	2.90181	0.400743	0.165628	24.9
SR2N	3.0	796	1677.5297	1.400319	3.33900	1.073520	0.106841	7.63
SR2N	4.0	664	1251.2665	0.993549	3.17614	0.715030	0.137892	13.9
SR1N	2.0	777	1314.5610	1314.561	3.12914	0.592821	0.288321	28.04
SR1N	3.0	639	1688.4160	1.37458	3.25649	1.050493	0.114695	8.344
SR1N	4.0	866	1711.6079	1.24370	2.90652	0.911062	0.098760	7.94

3.1 Effect of the impregnation ratio on the iodine index of activated carbons produced

The iodine index measures the porosity of pores of size ≥ 1.0 nm [22, 23]. Haimour and Emeish [12] proved by that there is a correlation between the iodine index and the specific surface. Figure 1 shows that the maximum iodine value of 893 $mg.g^{-1}$ is obtained in the SR series 2N and for the orthophosphoric acid impregnation ratio Xp = 2.5. For this series, the iodine value increases from 827 $mg.g^{-1}$ to 893 $mg.g^{-1}$ when Xp increases from 1.5 to 2.5, then decreases from 893 $mg.g^{-1}$ to 700 $mg.g^{-1}$ when Xp increases from 2.5 to 4.

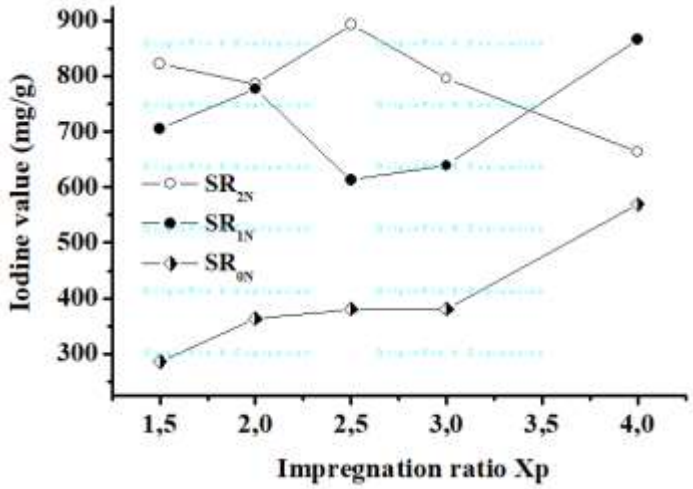

Figure 1: Effect of impregnation ratio Xp on iodine number of activated carbon for rate dilution of 25% and carbonization temperature of 500 °C

The lowest iodine index values are obtained for activated carbons in the SR_{0N} series. For activated carbons in this series (SR_{0N}), the iodine index increases from 280 to 380 $mg.g^{-1}$ when the orthophosphoric acid impregnation ratio Xp increases from 1.5 to 2.5, then remains constant until Xp=3, before reaching the maximum iodine index of 569 $mg.g^{-1}$ for Xp = 4. It is also noted that this maximum iodine index of activated carbons from the SR0N series is lower than the minimum iodine indices of the ACs from the SR1N and SR2N series (Figure 1).

In the SR series1N, the maximum iodine value of 866 $mg.g^{-1}$ is obtained for activated carbon at the orthophosphoric acid impregnation ratio Xp = 4. For the same orthophosphoric acid impregnation ratio (Xp = 4), and using rice bran pretreated with 1 N soda, Yun *et al.* [24] reported an optimum specific surface area S_{BET} = 2028 m^2/g for the activated carbon obtained. On the other hand, studies conducted by Liou and Wu [25], for the preparation of activated carbon from 1 N soda pretreated rice bran followed by activation with phosphoric acid H_3PO_4, resulted in the optimum iodine value at the impregnation ratio Xp equal to 2.

In their study, Wang *et al.* [20] developed a technique for the preparation of a so-called "hydrochars" activated carbon. Using as a precursor, rice bran pre-treated with 1 N sodium hydroxide solution; with activation with H_3PO_4 and carbonisation at 500 °C, this group of researchers showed that the optimum specific surface of this activated carbon, SB.E.T = 2700 m^2/g corresponds to the impregnation ratio Xp = 2.5.

3.2 Adsorption/desorption isotherms for activated carbons

The adsorption/desorption isotherm of N_2 on an adsorbent provides qualitative information on the adsorption mechanism and porosity of the adsorbent [26].

Examination of figures 2, 3 and 4 generally indicates a progressive adsorption of nitrogen on carbons in the range of relative pressures P/P_0 from 0 to 0.3. As a result, multilayers are formed in the pores of these activated carbons from low relative pressures. This type of behaviour reflects the existence of strong intermolecular interactions compared to the interaction between the molecules and the solid, hence the almost horizontal plateau for P/P_0 ranging from 0.3 to 0.7 that some isotherms present.

The nitrogen adsorption/desorption isotherms 2 on activated carbons (Figures 2, 3 and 4), regardless of the series, show a hysteresis loop at a relative pressure greater than 0.4. This characterizes the type IV isotherm [27]. It therefore follows that activated carbons are very mesoporous. The hysteresis loop observed is of type H_3/B according to the classifications of I.U.P.A.C and De Boer respectively [27, 28]. It is therefore mainly due to the slit-shaped pores. Also, most of these isotherms show a large increase in the slope at large relative pressures ($P/P_0 > 0.8$), which is attributed to the development of larger mesopores as reported by Yang and

Qiu [26]. This large increase in slope at relative pressures $P/P_0 > 0.8$ and which is particularly noticeable with the SR series activated coals 2N, is due to capillary condensation in the mesopores [6, 29]. Also, the high slope at these large relative pressures ($P/P_0 > 0.8$) is attributed to the development of larger pores [26].

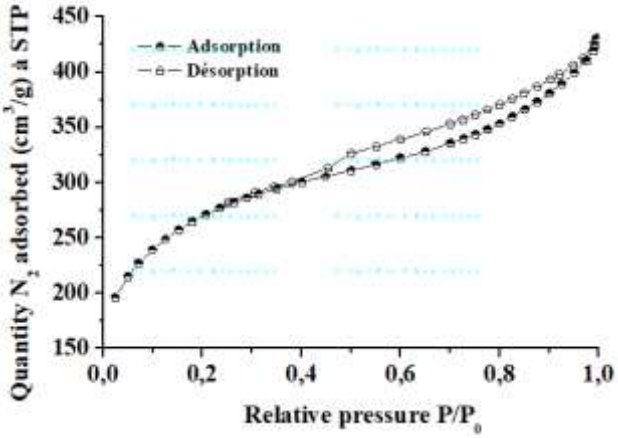

Figure 2: Adsorption/desorption isotherm for N_2 at 77 K on SR activated carbon0N - Xp = 4

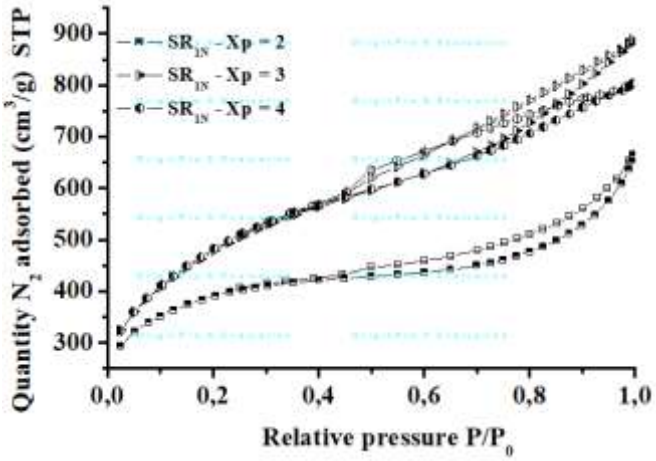

Figure 3: Adsorption/desorption isotherms for N_2 at 77 K on activated carbons from the SR series1N

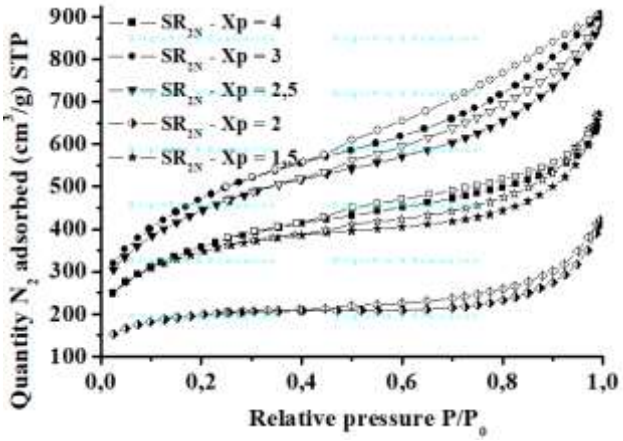

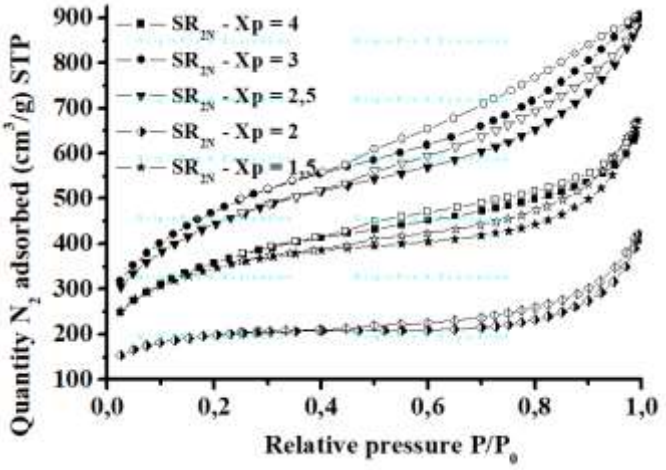

Figure 4: Adsorption/desorption isotherms for N2 at 77 K on activated carbons from the SR series2N.

3.3 Effect of the impregnation ratio on the adsorption capacity of N_2 on activated carbons

The nitrogen N_2 adsorption/desorption isotherms on activated carbons from the SR series1N (figures 3), indicate that the adsorption capacity of activated carbons increases with the ratio (rate) of impregnation with orthophosphoric acid Xp. Thus, the development of porosity is closely linked to the impregnation rate. Similar results have been reported by some research groups, including Sun and Paul, Prahas *et al*. [30, 31]. Furthermore, the isotherms of activated carbons obtained with orthophosphoric acid impregnation ratios Xp = 3 and 4 from this SR series 1N completely overlap at relative pressures ($P/P^0 < 0.7$). It should be pointed out that the isotherm of the activated carbon prepared with impregnation ratio Xp = 2 shows a plateau for relative pressures (P/P^0) ranging from 0.3 to 0.7, which is justified by the greater presence of micropores in this activated carbon compared to the other two in the same series (those prepared with ratios Xp = 3 and Xp = 4). In the SR series 2N, the activated carbon with an impregnation ratio Xp = 2.0 has the lowest nitrogen adsorption capacity with the most marked presence of micropores (Figure 4). Indeed, the isotherm of the latter presents an almost horizontal plateau for relative pressures P/P^0 ranging from 0.2 to 0.8. For high pressures ($P/P^0 > 0.8$), a greater adsorption of gas is observed, as shown by the activated carbons Xp = 1.5; 2.5 and especially that of the impregnation ratio Xp = 3 of this SR series 2N.

3.4 Effect of impregnation ratio Xp on specific surface area and total pore volume

Indeed, the graph obtained by the values of the first member of the BET equation as a function of p/P^0 makes it possible to determine the specific surface. The straight line obtained with slope $\frac{C_{BET^{-1}}}{V_{m1}.C_{BET}}$ and intercept $\frac{1}{V_{m1}.C_{BET}}$ allow the determination of the constants V_{ads} and C_{BET}. The S_{BET} specific surface and V can be determined from Qm.

3.4.1 Case of SR series activated carbons1N

Figure 5 shows the evolution of the specific surface area S_{BET} and the total pore volume V_T of activated carbons from the SR series1N. For activated carbons of the SR series1N, the specific surface area S_{BET} increases with the impregnation ratio Xp, and goes from 1314.7 to 1771.6 m^2/g when the impregnation ratio Xp goes from 2 to 4. As for the total pore volume V_T, the highest value is 1.374 cm^3/g and corresponds to the impregnation ratio Xp = 3. The largest mesoporous volume $V_{méso}$ for this SR series 1N also corresponds to

this impregnation ratio Xp = 3 (table 2). On the other hand, the volume Vμ of the micropores decreases with the increase of the impregnation ratio (table 2). The activated carbon with the impregnation ratio Xp = 4 designated CS1 has the smallest pore diameter (Dp = 2.9 nm) in this series SR1N.

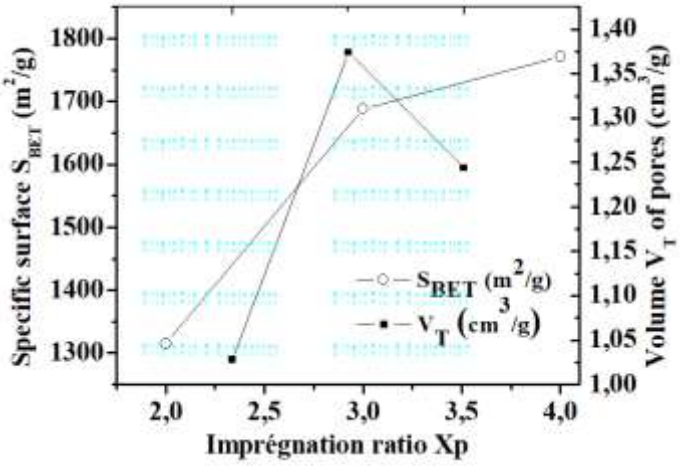

Figure 5: Specific surface area SBET and total volume VT as a function of the impregnation ratio SR activated carbons1N

3.4.2 Case of SR series activated carbons2N

Examination of Figure 6 shows that both parameters (specific surface area S_{BET} and the total pore volume V_T) evolve in the same direction. For ratios ranging from 1.5 to 3, the surface area S_{BET} increases, whereas the growth of the specific surface area is only observed for the range of impregnation ratios from 1.5 to 2.5.

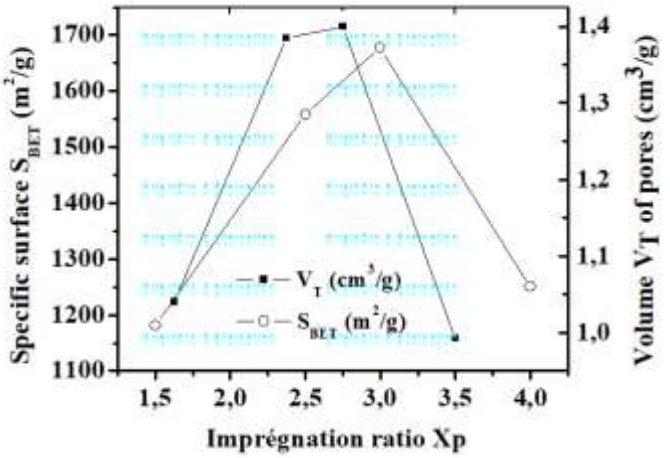

Figure 6: Specific surface area S_{BET} and total volume V_T as a function of the activated carbon impregnation ratio SR_{2N}

3.5 Pore size distribution of activated carbons SR1N and SR2N

The pore size distribution (PSD) is the most important aspect for the characterization of the structural (porous) heterogeneity of sorbents. For this study, the DTP pore size distribution of the elaborated activated carbons, determined using the BJH model, is presented in Table 2.

Table 2 shows the evolution of the specific surface and the iodine index of activated carbons SR_{2N} and SR_{1N} for impregnation ratios ranging from 1.5 to 4 for a dilution ratio of 50% and a carbonization temperature of 500 °C. Of the four different ways commonly used to represent the pore size distribution (PSD), these are:

1. the cumulative specific pore volume (larger or smaller) in relation to the pore size;
2. incremental specific pore volume versus pore size;
3. the differential pore volume (dV/dD) in relation to the pore size; and
4. the log differential of pore volume (dV/dlogD) as a function of pore size.

It emerges from this table that the SR carbons have developed a dominant mesoporous character with the V_{meso}/V_T (%) ratio ranging from 60.2 to 76.7. This observation is consistent with the adsorption/desorption isotherms of activated carbons in these series. The lowest V_{meso}/V_T ratio of 60.2% corresponds to the activated carbon with an impregnation ratio Xp = 4 in the SR_{0N} series,

Figures 7(a) and 7(b) illustrate the DTP pore size distribution of activated carbons from the SR series1N. Examination of the figures 7a and 7b highlights pore volume peaks mainly at pore diameters Dp of about 1.7 nm, 3 nm and 6.5 nm. For larger pore diameters (Dp >10 nm), pore volume peaks appeared around pore diameters of 30 and 50 nm.

Figures 8(a) and 8(b) illustrate the DTP pore size distribution of activated carbons from the SR series 2N. Figure 8(a) shows pore volume peaks around average pore diameters Dp = 2 nm. Other peaks are also observed for pore diameters greater than or equal to 2 nm (Dp ≥2). Furthermore, for larger diameter ranges, ranging from 50 to 100 nm, (Figure 8(b)), other peaks appeared.

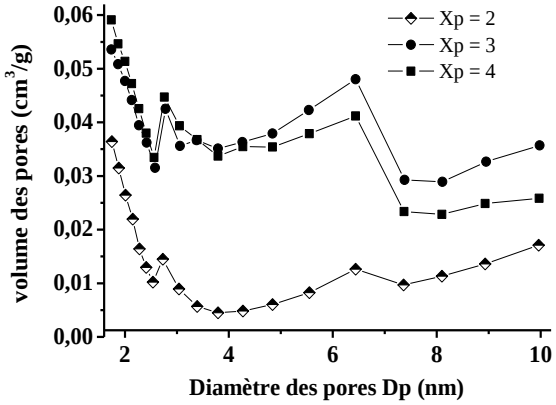

Figure 7(a): Size distribution of narrow mesopores (1,7 < Dp ≤ 10 nm) of SR1N series activated carbons, by B.J.H model

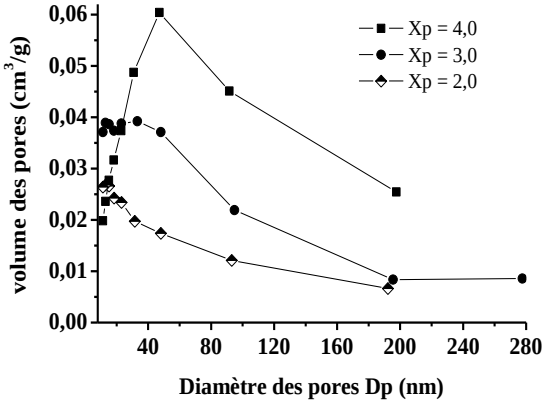

Figure 7(b): Size distribution of narrow mesopores (Dp > 10 nm) of SR1N series activated carbons, by B.J.H model

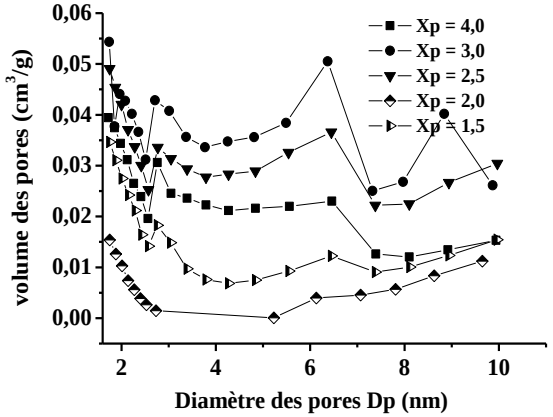

Figure 8(a): Size distribution of narrow mesopores (1,7 < Dp ≤ 10 nm) of SR2N series activated carbons, by B.J.H model

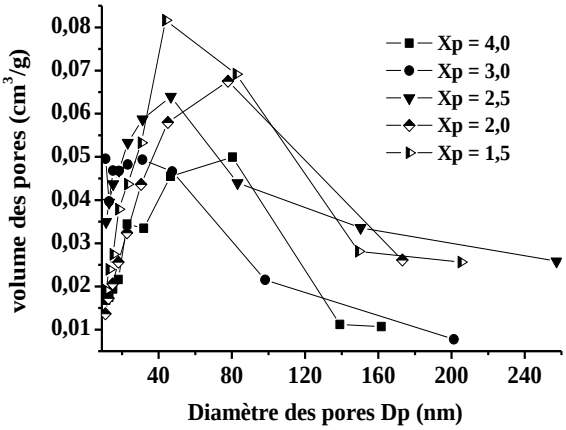

Figure 8(b): Size distribution of narrow mesopores (Dp > 10 nm) of SR2N series activated carbons by B.J.H model

The pore size distribution (figures 7 and 8) of activated carbons from the SR1N and SR2N series confirmed the mesoporous character of these activated carbons in accordance with the I.U.P.A.C. classification relating to pore typology. Indeed, the peaks of the pore volumes are mainly located in the pore diameter range from 2 to 50 nm.

The different activated carbons prepared from rice bran in the present study are characterized by their mesoporosity ($V_{méso}$ /V_T > 60%). Due to the high ash content of rice bran [32], the presence of certain metal oxides in activated carbons prepared from this precursor has been observed [3]. Thus, during the elaboration of these activated carbons, these metal oxides fill and/or block the micropores; this partially explains their relatively low specific surface, their mesoporous character and consequently the high volume of the pores. This is the case, for example, of the SR series of carbons 0N. Similar results have been reported by certain groups of researchers, including Valix *et al*. [33]; Yun *et al*. [34] and Oh and Park [35], who have shown that lignocellulosic precursors with a high ash content, such as rice bran, soybean and rapeseed stalks, rice straw and cassava skin, tend to produce activated carbons with a dominant mesoporous character.

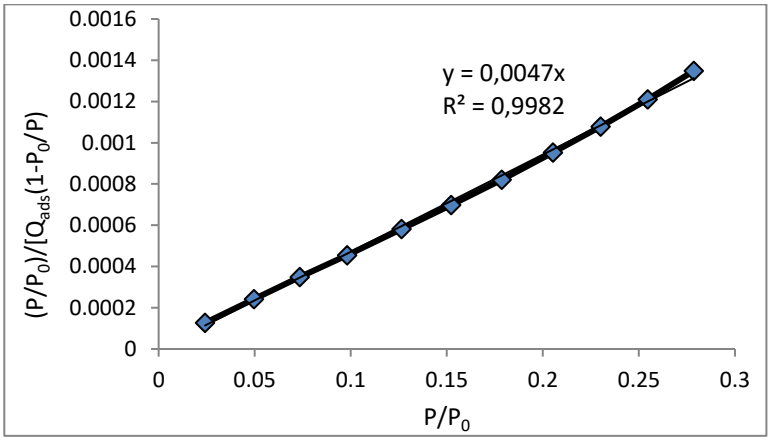

Figure 9: Linear transform of BET for the adsorption of N_2 on CA SR2N-Xp = 2.5

Barrett et al. [36] proposed a computational method to apply the Kelvin equation and explain the weakening of the adsorbed layer to obtain the pore size distribution from the adsorption isotherm data and is called the BJH method named after the initial promoters (Barrett, Joyner and Halenda) [36]. The limit of pore diameter that can be evaluated using the BJH theory of the adsorption branch is 1.7 nm because the Kelvin equation becomes invalid in micropores. This distribution is made along the desorption isotherm generally in the region where capillary condensation takes place (mesopores). This model complements Kelvin's approach by taking into account the variation in the number of adsorbed layers. The calculation of the mesopore distribution from the desorption branch gives information on the access pore diameters, while that calculated from the adsorption branch gives information on the actual pore diameter distribution.

The use of soda in the first stage of the process of preparing activated carbons of the SR1N and SR2N series made it possible to have a high porosity and large surface area (V_T > 0.9 cm^3 and S_{BET} > 1000 m^2/g), as shown in figures 5 and 6. The improvement in the textural properties of the coals in these series is justified by the fact that the phosphoric acid H_3PO_4 reacted directly with a precursor very rich in carbon. Indeed, the NaOH soda favored the reduction of impurities such as pigments, low molecular weight compounds and volatile matter. Similar results have been published by some research groups, including Basta and al [37] and Sudaryanto et al [38]. Furthermore, it was reported by Pankaj and al. [39] that the pretreatment of rice bran with NaOH soda eliminates the hemicellulose and cellulose and decreases its crystallinity, thus increasing the porosity and specific surface of the resulting activated carbon. It follows that the results of our work, which showed that the soda pre-treatment contributed to increase the iodine value of SR1N and SR2N activated carbons (thus their texture), are in agreement with the conclusions of the study conducted by Pankaj et al. [39]. The maximum iodine index of activated carbons in the SR0N series is lower than the minimum indices

of those in the SR1N and SR2N series. This allows us to conclude that the soda pre-treatment contributed to better iodine adsorption and therefore the development of microporosity. Similarly, as the concentration of the soda solution increases from 1 N to 2 N, the iodine values of the two carbons CS1 (SR1N - Xp = 4) and CS2 (SR2N - Xp = 2.5) are almost identical (866 and 893 mg/g respectively). It therefore appears that the increase in the concentration of soda for the pre-treatment of rice bran made it possible to reduce the impregnation ratio while presenting practically the same development of the microporosity of the activated carbons. The different activated carbons prepared from rice bran in the present study are characterized by their mesoporosity. Indeed, due to the high ash content of rice bran [39], it has been observed the presence of some metal oxides in activated carbons prepared from this precursor [3]. Thus, during the elaboration of these activated carbons, certain metal oxides fill and/or block the micropores; this partially explains their relatively low specific surface, their mesoporous character and consequently the high volume of the pores. This is the case, for example, of the SR series of 0N. Similar results have been reported by some groups of researchers including Valix and al [33], Yun and al [34] and Oh and Park [35] who showed that lignocellulosic precursors with high ash content, such as rice bran, soybean and rapeseed stalks, rice straw and cassava peel tend to produce CAs with higher mesopore volumes.

Conclusion

The two series of activated carbons SR1N and SR2N developed a mesoporous texture with average pore diameters ranging from 2.9 to 3.94 nm. For the SR1N series, the smallest average pore diameter (Dp = 2.9) corresponds to the impregnation ratio Xp = 4 with a specific surface S_{BET} = 17711.6 m^2/g.

Similarly for the SR series2N, the smallest average pore diameter is also at Dp = 2.9, but corresponds to Xp = 2.5 with a lower specific surface area, SBET of 917 m^2/g. It is observed that when the concentration of the soda solution is increased from 1 N to 2 N, the ratio of orthophosphoric acid impregnation Xp for the optimum iodine value increases from 4 to 2.5 in both series SR1N and SR2N. These optimum iodine values of the two series are almost identical. The corresponding activated carbons are: CS1 (SR1N, Xp = 4) and CS2 (SR2N, Xp = 2.5). An important property of adsorbents such as CA is the pore size distribution (PSD) which determines the fraction of the total pore volume accessible to molecules of a given size and shape. The optimal preparation process of activated carbon from mulberry shoot pruning was successfully achieved using a single factor method in this study. With an impregnation temperature of 80 °C, an impregnation ratio of 2:1 (v/w), an H_3PO_4 concentration of 50%, a pyrolysis temperature of 500 °C, and a pyrolysis time of 2 h, the activated carbon with improved iodine adsorption capacity and the yield was 887.35 mg/g and 38.12% respectively. Elemental analysis results and scanning electron microscopic micrographs indicated that pruning of the mulberry tree shoots are a good and cheap raw material for production activated carbon.

References

[1]. Romero-Anaya AJ, Ouzzine M, Lillo-Rodenas MA, Linares-Solano A (2014). Spherical carbons: Synthesis, characterization and activation processes. Carbon, 68:296–307.

[2]. Angin D (2014). Production and characterization of activated carbon from sour cherry stones by zinc chloride. Fuel, 115:804–811.

[3]. Konstantinou M, Pashalidis I (2010). Competitive sorption of Cu (II) and Eu (III) ions on olive-cake carbon in aqueous solutions—a potentiometric study. Adsorption, 16:167–171.

[4]. Jaramillo J, Álvarez PM, Gomez-Serrano V (2010). Oxidation of activated carbon by dry and wet methods: Surface chemistry and textural modifications. Fuel Processing Technology, 91:1768–1775.

[5]. Romero-Anaya AJ, Ouzzine M, Lillo-Rodenas MA, Linares-Solano A (2014). Spherical carbons: Synthesis, characterization and activation processes. Carbon, 68:296–307.

[6]. Angin D (2014). Production and characterization of activated carbon from sour cherry stones by zinc chloride. Fuel, 115:804–811.

[7]. Konstantinou M, Pashalidis I (2010). Competitive sorption of Cu (II) and Eu (III) ions on olive-cake carbon in aqueous solutions—a potentiometric study. Adsorption, 16:167–171.
[8]. Jaramillo J, Álvarez PM, Gomez-Serrano V (2010). Oxidation of activated carbon by dry and wet methods: Surface chemistry and textural modifications. Fuel Processing Technology, 91:1768–1775.
[9]. Jordá-Beneyto M, Suárez-García F, Lozano-Castello D, Cazorla-Amorós D, Linares-Solano A (2007). Hydrogen storage on chemically activated carbons and carbon nanomaterials at high pressures. Carbon, 45:293–303.
[10]. Reddy KSK, Al Shoaibi A, Srinivasakannan C (2012). A comparison of microstructure and adsorption characteristics of activated carbons by CO2 and H3PO4 activation from date palm pits. New Carbon Materials, 27:344–351.
[11]. Jo WK, Shin SH, Hwang ES (2011). Removal of dimethyl sulfide utilizing activated carbon fiber-supported photocatalyst in continuous-flow system. Journal of Hazardous Materials, 191:234–239.
[12]. Daud WMAW, Houshamnd AH (2010). Textural characteristics, surface chemistry and oxidation of activated carbon. Journal of Natural Gas Chemistry, 19:267–279.
[13]. Tseng HH, Wey MY (2006). Effects of acid treatments of activated carbon on its physiochemical structure as a support for copper oxide in DeSO2 reaction catalysts. Chemosphere, 62:756–766.
[14]. Tchakala I, Bawa LM, Djaneye-Boundjou G, Doni KS, Nambo P (2012). Optimisation du procédé de préparation des Charbons Actifs par voie chimique (H 3 PO 4) à partir des tourteaux de Karité et des tourteaux de Coton. International Journal of Biological and Chemical Sciences, 6:461–478.
[15]. Tchakala I, Alfa-Sika MS-L, Bafai DD, Kodom T, Bawa ML, Djaneye-Boundjou G (2019). Etude d'adsorption du phénol, du 4-chlorophénol et du 4-nitrophénol sur deux charbons actifs préparés à partir des tourteaux de karité (CA-K) et des graines de coton (CA-C): étude cinétique. Journal de la Société Ouest-Africaine de Chimie, 47:40–51.
[16]. Haimour NM, Emeish S (2006). Utilization of date stones for production of activated carbon using phosphoric acid. Waste Management, 26:651–660.
[17]. Jagtoyen M, Derbyshire F (1998). Activated carbons from yellow poplar and white oak by H_3PO_4 activation. Carbon, 36:1085–1097.
[18]. Guo Y, Rockstraw DA (2006). Physical and chemical properties of carbons synthesized from xylan, cellulose, and Kraft lignin by H_3PO_4 activation. Carbon, 44:1464–1475.
[19]. Ibrahim T, Moctar BL, Tomkouani K, Gbandi D-B, Victor DK, Phinthè N (2014). Kinetics of the adsorption of anionic and cationic dyes in aqueous solution by low-cost activated carbons prepared from sea cake and cotton cake. Am Chem Sci J, 4:38–57.
[20]. Al-Qaessi FAH (2001). Production of activated carbon from date stones using a fluidized-bed reactor. PhD Thesis, M. Sc. Thesis, University of Jordan, Amman, Jordan.
[21]. Ahmad AA, Hameed BH (2010). Effect of preparation conditions of activated carbon from bamboo waste for real textile wastewater. Journal of hazardous materials, 173:487–493.
[22]. Daud WMAW, Ali WSW (2004). Comparison on pore development of activated carbon produced from palm shell and coconut shell. Bioresource technology, 93:63–69.
[23]. N'djolosse K, Adoukonou-Sagbadja H, Maliki R, Kodjo S, Badou A, Adjovi RNA (2020). Performances agronomiques des arbres-mères d'anacardiers (Anacardium occidentale L.) sélectionnés dans les plantations paysannes au Bénin. International Journal of Biological and Chemical Sciences, 14:1536–1546.
[24]. Qu Y, Tian Y, Zou B, Zhang J, Zheng Y, Wang L, et al. (2010). A novel mesoporous lignin/silica hybrid from rice husk produced by a sol–gel method. Bioresource technology, 101:8402–8405.
[25]. Brunauer S, Emmett PH, Teller E (1938). Adsorption of gases in multimolecular layers. Journal of the American chemical society, 60:309–319.

[26]. Qureshi K, Bhatti I, Kazi R, Ansari AK (2008). Physical and chemical analysis of activated carbon prepared from sugarcane bagasse and use for sugar decolorisation. International Journal of Chemical and Biomolecular Engineering, 1:145–149.
[27]. Joseph CG, Zain HFM, Dek SF (2006). Treatment of landfill leachate in Kayu Madang, Sabah: textural and physical characterization (part 1). Malays J Anal Sci, 10:1–6.
[28]. Gundogdu A, Duran C, Senturk HB, Soylak M, Imamoglu M, Onal Y (2013). Physicochemical characteristics of a novel activated carbon produced from tea industry waste. Journal of Analytical and Applied Pyrolysis, 104:249–259.
[29]. Liou T-H, Wu S-J (2009). Characteristics of microporous/mesoporous carbons prepared from rice husk under base-and acid-treated conditions. Journal of hazardous materials, 171:693–703.
[30]. Yang J, Qiu K (2011). Development of high surface area mesoporous activated carbons from herb residues. Chemical engineering journal, 167:148–154.
[31]. Ure TAM, Butler LRP, L'vov BV, Rubeska I, Sturgeon R (1992). Nomenclature, symbols, units and their usage in spectrochemical analysis-XII. Terms related to electrothermal atomization (IUPAC Recommendations 1992). Pure and applied chemistry, 64:253–259.
[32]. De Boer JH, Van Den Heuvel A, Linsen BG (1964). Studies on pore systems in catalysts IV. The two causes of reversible hysteresis. Journal of Catalysis, 3:268–273.
[33]. Tien C Adsorption calculations and modeling. Butterworth-Heinemann; 1994.
[34]. Sun K, Chun Jiang J (2010). Preparation and characterization of activated carbon from rubber-seed shell by physical activation with steam. Biomass and bioenergy, 34:539–544.
[35]. Prahas D, Kartika Y, Indraswati N, Ismadji S (2008). Activated carbon from jackfruit peel waste by H_3PO_4 chemical activation: Pore structure and surface chemistry characterization. Chemical Engineering Journal, 140:32–42.
[36]. Reshad AS, Tiwari P, Goud VV (2018). Thermo-chemical conversion of waste rubber seed shell to produce fuel and value-added chemicals. Journal of the Energy Institute, 91:940–950.
[37]. Valix M, Cheung WH, McKay G (2004). Preparation of activated carbon using low temperature carbonisation and physical activation of high ash raw bagasse for acid dye adsorption. Chemosphere, 56:493–501.
[38]. Yun W, Hall IR (2004). Edible ectomycorrhizal mushrooms: challenges and achievements. Canadian Journal of Botany, 82:1063–1073.
[39]. Oh GH, Park CR (2002). Preparation and characteristics of rice-straw-based porous carbons with high adsorption capacity. Fuel, 81:327–336.
[40]. Barrett EP, Joyner LG, Halenda PP (1951). The determination of pore volume and area distributions in porous substances. I. Computations from nitrogen isotherms. Journal of the American Chemical society, 73:373–380.
[41]. Basta AH, Fierro V, El-Saied H, Celzard A (2009). 2-Steps KOH activation of rice straw: an efficient method for preparing high-performance activated carbons. Bioresource technology, 100:3941–3947.
[42]. Sudaryanto Y, Hartono SB, Irawaty W, Hindarso H, Ismadji S (2006). High surface area activated carbon prepared from cassava peel by chemical activation. Bioresource technology, 97:734–739.
[43]. Roy B, Brahma B, Ghosh S, Pankaj PK, Mandal G (2011). Evaluation of milk urea concentration as useful indicator for dairy herd management: A review. Asian J Anim Vet Adv, 6:1–19.